JET–P(92)82

D. Borba, M.F.F. Nave, F. Porcelli
and JET Team

The Non Linear Behaviour of Fishbones

The Non Linear Behaviour of Fishbones

D. Borba[1], M.F.F. Nave[2], F. Porcelli
and JET Team*

JET-Joint Undertaking, Culham Science Centre, OX14 3DB, Abingdon, UK

[1]*Association Euratom/IST-Centro de Fusao Nuclear fustituto Superior Tecnico, Lisboa Codex, Portugal*
[2]*LNETI, Sacavem, Portugal*
** See Annex*

Preprint of a paper to be submitted for publication in the proceedings of the
International School of Plasma Physics 'Piero Caldirola' (Varenna 1992)

The Non Linear Behavior of Fishbones

D.Borba,M.F.F.Nave* [1],F.Porcelli*
*Jet Joint Undertaking, Abingdon, Oxon, OX14 3EA, U.K.
Association Euratom/IST - Centro de Fusão Nuclear
Instituto Superior Tecnico , 1096 LISBOA Codex PORTUGAL

Abstract

Tokamak plasmas present many interesting non linear aspects. The fishbone instability is a good example of this kind of irregular and complex behavior. A simple heuristic non-linear model has been developed to study the fishbone repetition cycle. The model consists of two coupled non-linear differential equations, which describe the evolution of the mode amplitude and the resonant fast ion density as a function of time. This model predicts two forms of fishbones, i.e. short repetitive bursts as well as continuous oscillations. An extended model includes the slowing down of fast ions, two types of loss mechanisms (particle diffusion and ergodization of the fast ion orbits) and a periodic forcing term due to other MHD events, such as ELM's. This refined model allows more complex solutions which qualitatively reflect the irregular behavior sometimes observed in JET experimental data.

Introduction

Fishbones were first observed in the Princeton PDX tokamak in 1983 associated with the loss of fast particles /1/. These MHD central modes are observed in auxiliary heated JET discharges. They appear either in the form of repetitive bursts or as continuous oscillations of the poloidal magnetic field, soft x-rays signals and other diagnostics /2,3/. In this work a model for the non linear dynamics of this instability is developed and compared with recent JET experimental data. The model consists of two coupled non linear differential equations which describe the time evolution of MHD mode amplitude and of the fast ions density in NBI heated discharges. The model gives a relation between the amplitude and repetition time of the bursts. In addition, also the shape (i.e. burst vs continuous oscillations) and the mode amplitude are related to one another.

Simple Model

A simple heuristic non-linear model has been developed to study the fishbone repetition cycle /4,5/. In this model the two quantities that vary in time are the normalized mode amplitude, $A = \frac{|\tilde{B}_\theta|}{B_\theta}$, and the density of resonant ions n_h.

$$\frac{\partial A}{\partial t} = -\gamma_\eta A + \frac{\gamma_{mhd}}{n_0} n_h A \qquad (1)$$

$$\frac{\partial n_h}{\partial t} = S_h - \gamma_L n_{crit} A^\nu \qquad (2)$$

Assuming that the fast ion magnetic drift frequency and thermal ion diamagnetic frequency are comparable, we follow the analysis of Ref./5/, where the equation for the

[1] Permanent address LNETI, Sacavem, Portugal

mode amplitude (1) is obtain from linear theory. The growth rate is proportional to the density of resonant super-thermal ions and to the ideal stability parameter γ_{mhd}. γ_η is a damping term due to plasma resistivity. The equation for the density of the resonant ions (2) is obtained assuming that the constant source of ions S_h, is provided by auxiliary heating, γ_L is a loss rate and $n_{crit} = \frac{\gamma_\eta}{\gamma_{mhd}} n_0$ is the critical fast ion density threshold for the excitation of the instability (a definition of n_0 can be found in /5/). We consider two possibilities for the loss term proportional to A^ν: $\nu = 1$ corresponds to secular losses and $\nu = 2$ corresponds to losses resulting from orbit stochasticity /6/. The numerical solution of (1)-(2) is represented in Fig 1.

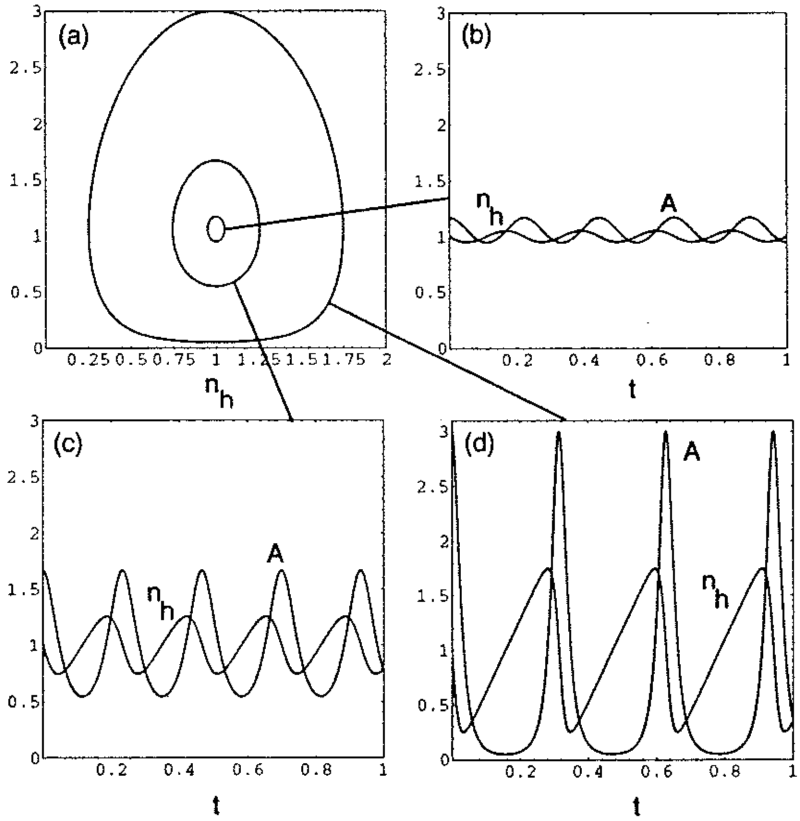

Fig 1 represents a numerical solution of the model equations for normalized model parameters ($\frac{\gamma_{mhd}}{n_0} = 15$,$\gamma_\eta = 15$,$S_h = 1.5$ and $\gamma_L n_{crit} = 1.5$). A,t and n_h are represented in units normalized to the fixed point ($A_0 = \frac{S_h}{\gamma_L n_{crit}} = 1$, $n_{h0} = n_{crit} = 1$). Realistic physical dimensions will be given in the last section. The phase-space trajectories are obtained for the initial conditions ($n_h = 1, A = 1, 1.6, 3$) in Fig 1 (a) and the respective time dependent solutions are shown in Fig 1 (b) (c) (d).

The dynamical system has a fixed point, $A_0 = \frac{S_h}{\gamma_L n_{crit}}$, $n_{h0} = n_{crit}$. Small perturbations near the fixed point correspond to continuous oscillations Fig (1b), while large trajectories in Fig (1a) correspond to bursting solutions shown in Fig (1d). Fig (1c) exhibits an intermediate case.

Introducing new variables an analytic solution for the phase-space trajectories can be obtained.

$$y = \log A \quad , \quad x = -\gamma_\eta + \frac{\gamma_{mhd}}{n_0} n_h \tag{3,4}$$

The system of differential equations in new variables is:

$$\dot{y} = x \quad , \quad \ddot{y} = \frac{\gamma_{mhd}}{n_0}(S_h - \gamma_L n_{crit} e^{\nu y}) \tag{5,6}$$

Defining the new variable around the fixed point $\bar{y} = -\frac{\log \frac{S_h}{\gamma_L n_{crit}}}{\nu} + y$ and $\Gamma = \frac{\gamma_{mhd}}{n_0} S_h$, we get a simple equation (7) for this dynamical system:

$$\ddot{\bar{y}} = \Gamma(1 - e^{\nu \bar{y}}) \tag{7}$$

Upon integration of (7), we obtain an expression for an effective potential, which rules the non-linear oscillator.

$$V_{eff} = \Gamma(\frac{e^{\nu \bar{y}}}{\nu} - \bar{y}) \tag{8}$$

the system of equations can be put in the Hamiltonian form:

$$H = T + V \quad , \quad T = \frac{\dot{\bar{y}}^2}{2} \quad , \quad V = \frac{\gamma_{mhd}}{n_0} S_h (\frac{e^{\nu \bar{y}}}{\nu} - \bar{y}) \tag{9,10,11}$$

and using the original variables (3),(4) we get an equation for the trajectories as function of the parameter H in phase-space:

$$H = \frac{(-\gamma_\eta + \frac{\gamma_{mhd}}{n_0} n_h)^2}{2} + \frac{\gamma_{mhd}}{n_0}(\frac{\gamma_L n_{crit} A^\nu}{\nu} - S_h \log A) \tag{12}$$

Perturbed Model

The simple model does not allow for the irregular behavior observed in most of the experimental data. However, a small perturbation of the simple model is sufficient in order to account for this irregular behavior. We propose the following modified model:

$$\frac{\partial A}{\partial t} = -\gamma_\eta A + \frac{\gamma_{mhd}}{n_0} n_h A \quad , \quad \frac{\partial n_h}{\partial t} = S_h - \gamma_L n_{crit} A^\nu - \Lambda n_h + \Omega Cos(\omega t) \tag{13,14}$$

In the equation for the evolution of the fast ion population, we have added a slowing down term proportional to Λ, and a sinusoidal forcing term with amplitude Ω and frequency ω. This forcing term is suggested by the experimental evidence of the modulation of the fast particle distribution function by other MHD events. This point is discussed further in the last Section. The solution of these equations is characterized by two regimes: a transient solution and a time asymptotic solution. The transient solution gives an irregular behavior as shown in Fig 2.

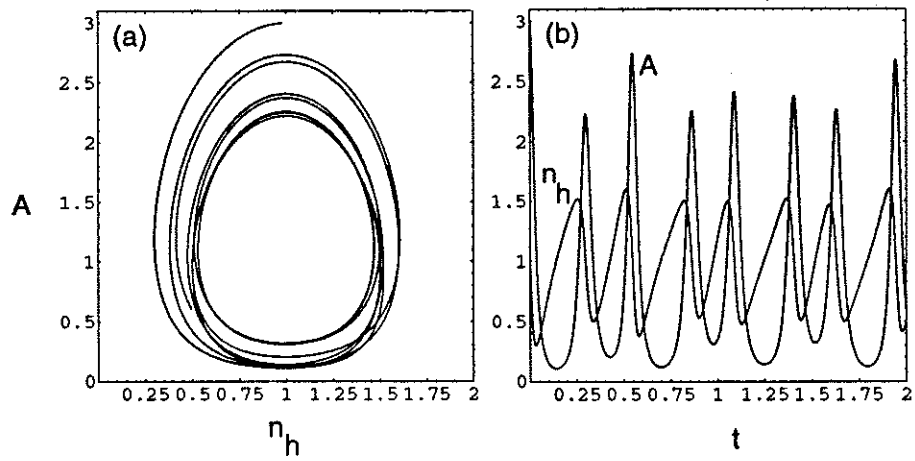

Fig 2 Transients solution of the perturbed model using normalized units. Phase-space trajectories shown in fig 2 (a) and time dependent solutions shown in fig 2 (b)

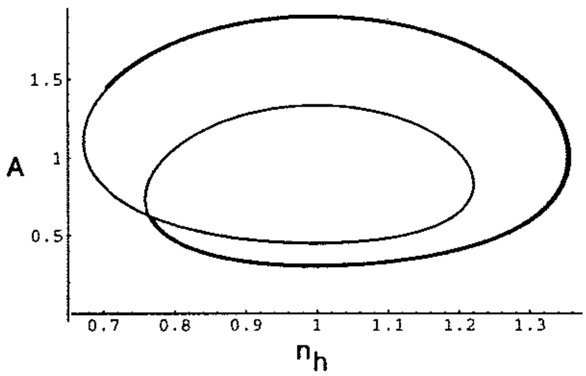

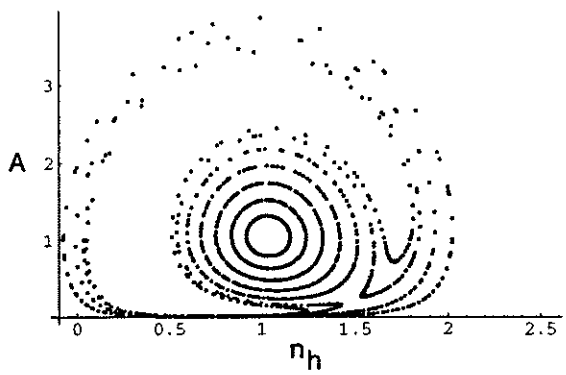

Fig 3 Time asymptotic solution of the perturbed model using normalized units.

Fig 4 Phase-space Poincaré section for a perturbed model resonant solution using normalized units.

The time asymptotic solution gives stable orbits which can become very complex. An example is the double orbit solution in phase-space shown in (Fig 3). If the forcing frequency is close to the repetition frequency of fishbones pertaining to the simple model, an island grows in the Poincaré section of the phase-space giving the complex resonant behavior shown in Fig 4.

Experimental data

The experimental observations of fishbones presented hereafter were obtained during the 1991/92 JET campaign with the magnetic pick-up coils. Fig 5 shows an example of fishbone bursts developing into continuous oscillations. The simple model predicts both behaviors. The observed transition from one behavior into the other can only be explained by the perturbed model.

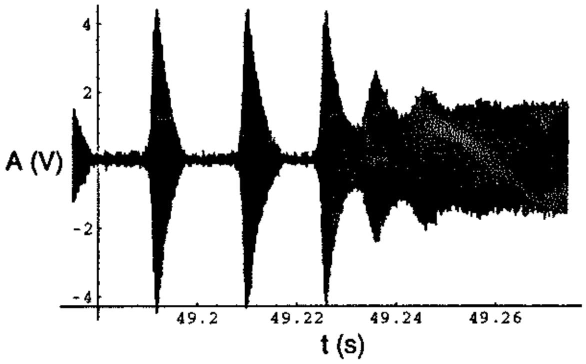

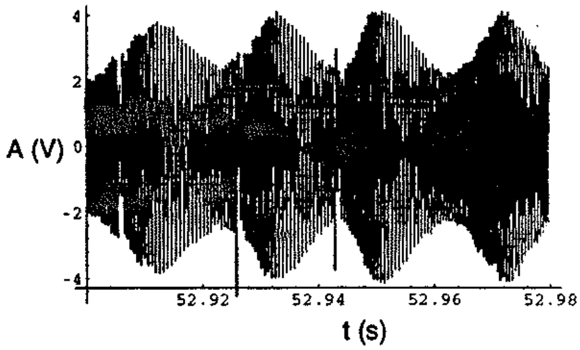

Fig 5 Fishbone bursts developing into continuous oscillations.
Fig 6 Small oscillations in amplitude around the continuous oscillations.

Small oscillations in amplitude around the continuous oscillations, which are predicted by the simple model are also seen in the experimental data (Fig 6). Large amplitude bursts can be fitted using the non-linear simple model. It is not possible to infer all parameters in the model by fitting to the experimental results, because we do not have direct information about the resonant ion population. However, it is possible to estimate some of the parameters from the fitting shown in Fig 7, which has been obtained using $\nu = 2$ and $\Gamma = 10^5 s^{-2}$ (see equation 7).

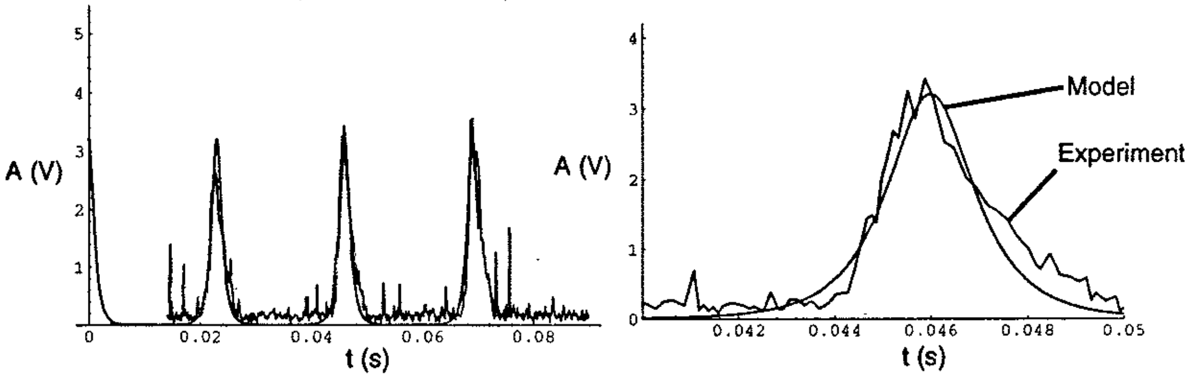

Fig 7 Fit using the simple non-linear model with $\nu = 2$ and $\Gamma = 10^5 s^{-2}$

This value of Γ is consistent with the parameters $\gamma_{mhd} \approx 10^4 s^{-1}$, $S_h \approx 10^{12} s^{-1} cm^{-3}$ and $n_0 \approx 10^{11} cm^{-3}$. This value of S_h can be obtained in a 10 MW NBI heated JET discharge for a plasma volume of the order of $100m^3$.

Usually fishbones appear either as a long continuous oscillation or as several periodic bursts, however Fig 8 shows a discharge where both behaviors appear in a very short period of time. During this period the ELM repetition time is very close to the fishbone cycle period. This gives a strong evidence that a resonant interaction between the fishbone dynamics and other MHD events in the plasma, such as Edge Localized Modes (ELM's), might be behind this behavior, as described by the perturbed model.

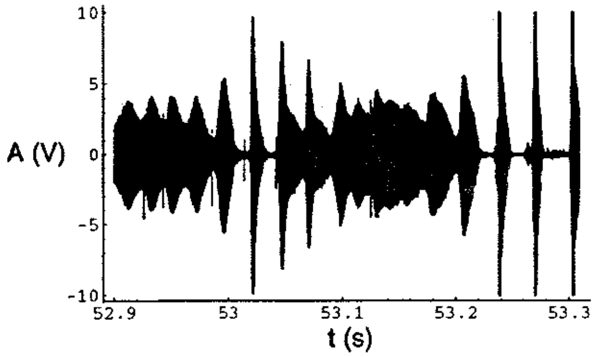

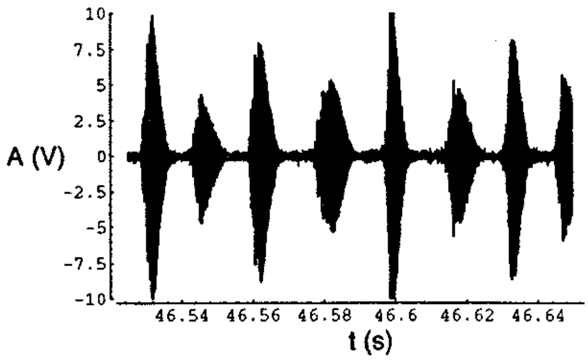

Fig 8 An example where both fishbone behaviors appear in a very short period of time. The much faster events observed in this plot are Edge Localized Modes (ELM's)

Fig 9 Period doubling in the fishbone cycle.

The dynamics of the island solution is similar to some experimental observations, with bursts turning into continuous oscillations and continuous oscillations turning into bursts periodically (Fig 8). Most of the experimental data show irregular burst behavior. Fig 9 shows period doubling in the fishbone cycle. The refined model allows similar solutions (Fig 3), but the mechanism and the condition for bifurcation in the non-linear oscillator has not yet been understood.

Conclusions

Quantitative and qualitative results in a complex subject, such as the interaction between supra-thermal ions and MHD modes, can be obtained studying the dynamics of fishbone instability using simple heuristic arguments. From the analysis using the simple model, it is clear that continuous oscillations and fishbone bursts observed in some experimental results are two different aspects of the same phenomena. The time scale of the instability is obtained from the simple model fitting to the experiment $\Gamma \approx 10^5 s^{-2}$ (see equation 7). Period doubling and irregular behavior are observed giving strong evidence of a non-linear dynamics.

References

/1/ McGuire,K Goldston,R Bell,M et al Phy.Rev.Lett 50 (1983) 891

/2/ Nave,M.F.F.,Campbell,D.J.,Joffrin,E et al. Nuclear Fusion 31(1991) 697

/3/ F.Nave et all Energetic Particles Driven Instabilities at JET , (1992 International conference on Plasma Physics, Innsbruck, 1992) vol.16 C, part I, p.439

/4/ Liu Chen,R B White, M N Rosenbluth Phy.Rev.Lett 52 (1984) 1122

/5/ Coppi,B. Porcelli,F. Phys.Rev.Lett.57 (1986) 2722, Coppi,B. Migliuolo,S. Porcelli,F. Phys.Fluids 31,1630 (1988)

/6/ R.B.White et al Phys. Fluids 26 (10) October 1983

Appendix I

THE JET TEAM

JET Joint Undertaking, Abingdon, Oxon, OX14 3EA, U.K.

J.M. Adams[1], B. Alper, H. Altmann, A. Andersen[14], P. Andrew, S.Ali-Arshad, W. Bailey, B. Balet, P. Barabaschi, Y. Baranov, P. Barker, R. Barnsley[2], M. Baronian, D.V. Bartlett, A.C. Bell, G. Benali, P. Bertoldi, E. Bertolini, V. Bhatnagar, A.J. Bickley, D. Bond, T. Bonicelli, S.J. Booth, G. Bosia, M. Botman, D. Boucher, P. Boucquey, M. Brandon, P. Breger, H. Brelen, W.J. Brewerton, H. Brinkschulte, T. Brown, M. Brusati, T. Budd, M. Bures, P. Burton, T. Businaro, P. Butcher, H. Buttgereit, C. Caldwell-Nichols, D.J. Campbell, D. Campling, P. Card, G. Celentano, C.D. Challis, A.V.Chankin[23], A. Cherubini, D. Chiron, J. Christiansen, P. Chuilon, R. Claesen, S. Clement, E. Clipsham, J.P. Coad, I.H. Coffey[24], A. Colton, M. Comiskey[4], S. Conroy, M. Cooke, S. Cooper, J.G. Cordey, W. Core, G. Corrigan, S. Corti, A.E. Costley, G. Cottrell, M. Cox[7], P. Crawley, O. Da Costa, N. Davies, S.J. Davies[7], H. de Blank, H. de Esch, L. de Kock, E. Deksnis, N. Deliyanakus, G.B. Denne-Hinnov, G. Deschamps, W.J. Dickson[19], K.J. Dietz, A. Dines, S.L. Dmitrenko, M. Dmitrieva[25], J. Dobbing, N. Dolgetta, S.E. Dorling, P.G. Doyle, D.F. Düchs, H. Duquenoy, A. Edwards, J. Ehrenberg, A. Ekedahl, T. Elevant[11], S.K. Erents[7], L.G. Eriksson, H. Fajemirokun[12], H. Falter, J. Freiling[15], C. Froger, P. Froissard, K. Fullard, M. Gadeberg, A. Galetsas, L. Galbiati, D. Gambier, M. Garribba, P. Gaze, R. Giannella, A. Gibson, R.D. Gill, A. Girard, A. Gondhalekar, D. Goodall[7], C. Gormezano, N.A. Gottardi, C. Gowers, B.J. Green, R. Haange, A. Haigh, C.J. Hancock, P.J. Harbour, N.C. Hawkes[7], N.P. Hawkes[1], P. Haynes[7], J.L. Hemmerich, T. Hender[7], J. Hoekzema, L. Horton, J. How, P.J. Howarth[5], M. Huart, T.P. Hughes[4], M. Huguet, F. Hurd, K. Ida[18], B. Ingram, M. Irving, J. Jacquinot, H. Jaeckel, J.F. Jaeger, G. Janeschitz, Z. Jankowicz[22], O.N. Jarvis, F. Jensen, E.M. Jones, L.P.D.F. Jones, T.T.C. Jones, J-F. Junger, F. Junique, A. Kaye, B.E. Keen, M. Keilhacker, W. Kerner, N.J. Kidd, R. Konig, A. Konstantellos, P. Kupschus, R. Lässer, J.R. Last, B. Laundy, L. Lauro-Taroni, K. Lawson[7], M. Lennholm, J. Lingertat[13], R.N. Litunovski, A. Loarte, R. Lobel, P. Lomas, M. Loughlin, C. Lowry, A.C. Maas[15], B. Macklin, C.F. Maggi[16], G. Magyar, V. Marchese, F. Marcus, J. Mart, D. Martin, E. Martin, R. Martin-Solis[8], P. Massmann, G. Matthews, H. McBryan, G. McCracken[7], P. Meriguet, P. Miele, S.F. Mills, P. Millward, E. Minardi[16], R. Mohanti[17], P.L. Mondino, A. Montvai[3], P. Morgan, H. Morsi, G. Murphy, F. Nave[27], S. Neudatchin[23], G. Newbert, M. Newman, P. Nielsen, P. Noll, W. Obert, D. O'Brien, J. O'Rourke, R. Ostrom, M. Ottaviani, S. Papastergiou, D. Pasini, B. Patel, A. Peacock, N. Peacock[7], R.J.M. Pearce, D. Pearson[12], J.F. Peng[26], R. Pepe de Silva, G. Perinic, C. Perry, M.A. Pick, J. Plancoulaine, J-P. Poffé, R. Pohlchen, F. Porcelli, L. Porte[19], R. Prentice, S. Puppin, S. Putvinskii[23], G. Radford[9], T. Raimondi, M.C. Ramos de Andrade, M. Rapisarda[29], P-H. Rebut, R. Reichle, S. Richards, E. Righi, F. Rimini, A. Rolfe, R.T. Ross, L. Rossi, R. Russ, H.C. Sack, G. Sadler, G. Saibene, J.L. Salanave, G. Sanazzaro, A. Santagiustina, R. Sartori, C. Sborchia, P. Schild, M. Schmid, G. Schmidt[6], H. Schroepf, B. Schunke, S.M. Scott, A. Sibley, R. Simonini, A.C.C. Sips, P. Smeulders, R. Smith, M. Stamp, P. Stangeby[20], D.F. Start, C.A. Steed, D. Stork, P.E. Stott, P. Stubberfield, D. Summers, H. Summers[19], L. Svensson, J.A. Tagle[21], A. Tanga, A. Taroni, C. Terella, A. Tesini, P.R. Thomas, E. Thompson, K. Thomsen, P. Trevalion, B. Tubbing, F. Tibone, H. van der Beken, G. Vlases, M. von Hellermann, T. Wade, C. Walker, D. Ward, M.L. Watkins, M.J. Watson, S. Weber[10], J. Wesson, T.J. Wijnands, J. Wilks, D. Wilson, T. Winkel, R. Wolf, D. Wong, C. Woodward, M. Wykes, I.D. Young, L. Zannelli, A. Zolfaghari[28], G. Zullo, W. Zwingmann.

PERMANENT ADDRESSES

1. UKAEA, Harwell, Didcot, Oxon, UK.
2. University of Leicester, Leicester, UK.
3. Central Research Institute for Physics, Budapest, Hungary.
4. University of Essex, Colchester, UK.
5. University of Birmingham, Birmingham, UK.
6. Princeton Plasma Physics Laboratory, New Jersey, USA.
7. UKAEA Culham Laboratory, Abingdon, Oxon, UK.
8. Universidad Complutense de Madrid, Spain.
9. Institute of Mathematics, University of Oxford, UK.
10. Freien Universität, Berlin, F.R.G.
11. Royal Institute of Technology, Stockholm, Sweden.
12. Imperial College, University of London, UK.
13. Max Planck Institut für Plasmaphysik, Garching, FRG.
14. Risø National Laboratory, Denmark.
15. FOM Instituut voor Plasmafysica, Nieuwegein, The Netherlands.
16. Dipartimento di Fisica, University of Milan, Milano, Italy.
17. North Carolina State University, Raleigh, NC, USA
18. National Institute for Fusion Science, Nagoya, Japan.
19. University of Strathclyde, 107 Rottenrow, Glasgow, UK.
20. Institute for Aerospace Studies, University of Toronto, Ontario, Canada.
21. CIEMAT, Madrid, Spain.
22. Institute for Nuclear Studies, Otwock-Swierk, Poland.
23. Kurchatov Institute of Atomic Energy, Moscow, USSR
24. Queens University, Belfast, UK.
25. Keldysh Institute of Applied Mathematics, Moscow, USSR.
26. Institute of Plasma Physics, Academica Sinica, Hefei, P. R. China.
27. LNETI, Savacem, Portugal.
28. Plasma Fusion Center, M.I.T., Boston, USA.
29. ENEA, Frascati, Italy.

At 1st July. 1992